

## Concentration Dependence of the Collective Dynamics of Swimming Bacteria

Andrey Sokolov,<sup>1,2</sup> Igor S. Aranson,<sup>1</sup> John O. Kessler,<sup>3</sup> and Raymond E. Goldstein<sup>3,4</sup>

<sup>1</sup>Argonne National Laboratory, 9700 South Cass Avenue, Argonne, Illinois 60439, USA

<sup>2</sup>Illinois Institute of Technology, 3101 South Dearborn Street, Chicago, Illinois 60616, USA

<sup>3</sup>Department of Physics, Program in Applied Mathematics, and BIO5 Institute, University of Arizona, Tucson, Arizona 85721, USA

<sup>4</sup>Department of Applied Mathematics and Theoretical Physics, University of Cambridge, Wilberforce Road, Cambridge CB3 0WA, United Kingdom

(Received 7 August 2006; published 11 April 2007)

At concentrations near the maximum allowed by steric repulsion, swimming bacteria form a dynamical state exhibiting extended spatiotemporal coherence. The viscous fluid into which locomotive energy of individual microorganisms is transferred also carries interactions that drive the coherence. The concentration dependence of correlations in the collective state is probed here with a novel technique that herds bacteria into condensed populations of adjustable concentration. For the particular thin-film geometry employed, the correlation lengths vary smoothly and monotonically through the transition from individual to collective behavior.

DOI: [10.1103/PhysRevLett.98.158102](https://doi.org/10.1103/PhysRevLett.98.158102)

PACS numbers: 87.16.-b, 05.65.+b, 87.17.Jj

The past decade has seen growing interest in the dynamical properties of interacting, self-propelled organisms, such as bacteria, sperm cells, fish, marching locusts, etc. [1–5]. This “many-body problem” was motivated by phenomena in biology, but is now recognized to encompass nonequilibrium statistical mechanics and nonlinear dynamics [6–10]. A fundamental issue is the nature of possible transitions to collective motion and the relation between highly simplified “flocking” models, which are based on local interactions between elements, and the phenomenon of collective swimming in which nonlocal hydrodynamic interactions are obviously important.

Suspensions of swimming bacteria serve as model systems for this problem. Experiments on *E. coli* in soaplike thin fluid films [1] showed that small whorls and jets of cooperative swimming produced greatly enhanced diffusion and even superdiffusion [11] of passive tracers, establishing the idea of a “bacterial bath” akin to the molecular bath responsible for Brownian motion. Even in the restricted geometry of a thin film it was clear that recurring, coherent structures were important on scales exceeding those of individual bacteria. More recent experiments [2–4] and simulations [12] have demonstrated that the correlation length of collective motion can exceed the size of individual cells by more than an order of magnitude, and the collective flow speeds (of the order 50–100  $\mu\text{m}/\text{sec}$ ) similarly exceed the speed of individual bacteria (about 15–20  $\mu\text{m}/\text{sec}$ ). This collective swimming is found at sufficiently high number density (or volume fraction) of the microorganisms; dilute suspensions show no collective flow and the correlation length is comparable to the size of a bacterium. These works also highlighted hydrodynamic interactions between bacteria as the origin of collective flows, in contrast to the irrelevance of advective motion compared to diffusion at the scale of individual cells.

In light of the developments outlined above, two key questions involving collective dynamics can be identified. How do spatiotemporal correlations depend on the concentration of microorganisms? How can their concentration be managed as a control parameter? Here we address these questions by reporting experimental studies of collective bacterial swimming in thin-film geometry utilizing a new technique to adjust the number density of bacteria of a given experiment. This allows measurement of the correlation length and the mean swimming speed over a range of densities *with a single bacterial colony*, greatly reducing statistical fluctuations due to the inherent physiological differences between colonies. In contrast with the earliest phenomenological theories [6–10], we find only a gradual increase of the correlation length with increasing density, and no sharp transition. We propose that this can be explained as a noise-induced smearing of a dynamical phase transition, the main source of noise being that due to strong fluctuations in the orientation of individual bacteria [1].

Experiments were conducted on suspensions of strains 1085 and YB886 of *Bacillus subtilis*, a peritrichously flagellated rod-shaped bacterium  $\sim 4 \mu\text{m}$  long and with a diameter of  $\sim 0.7 \mu\text{m}$ . Spores stored on agar or sand were used to inoculate nutrient medium. The suspension of grown cells was then washed and centrifuged. Our experimental setup, shown in Fig. 1, is similar to that used by Wu and Libchaber [1], but has a number of important modifications. A small drop of bacterial suspension is placed between four supporting, movable fibers: two Platinum (Pt) wires (to exclude contamination of the film) and two dielectric fibers. The drop was then stretched between the fibers up to the necessary thickness (about  $1 \mu\text{m}$ ) by pulling all the fibers apart with a control screw. The film was placed in a container with air saturated with water to minimize evaporation. Unlike previous experiments on *E. coli* [1], no additional surfactant was used to stabilize the fluid

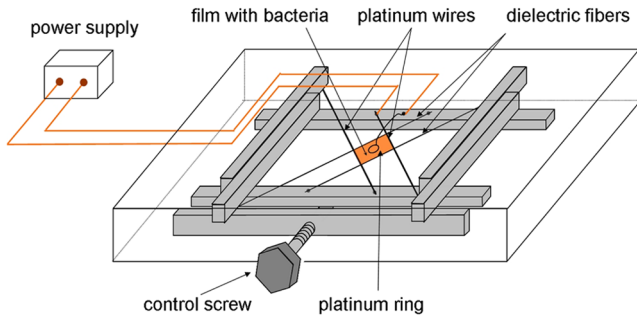


FIG. 1 (color online). Schematics of experimental setup. A thin film containing bacteria spans two adjustable Pt wires and two dielectric fibers and is stretched by a control screw. Electric current is transmitted between the Pt wires and a small Pt ring lowered onto the film. The cell is within a humidity controlled chamber.

film. Instead, the metabolic products secreted by *B. subtilis* created the necessary surface tension and elasticity to maintain the film during the course of an experiment, typically several minutes. After that, the film either ruptured, or the secreted products solidified and motion ceased to exist. Images were obtained with a video camera operating at 100 frame/s, equipped with a high-resolution, long working distance microscope objective. Image processing was performed by custom-designed software based on Matlab toolboxes. Working with a monolayer film of bacteria allows us to identify, count, and track each and every cell in the field of view.

In order to adjust the density of bacteria (the “filling fraction”  $\rho$ ) in the course of one experiment, a small platinum ring (diameter  $\sim 1$  mm) was gently lowered onto the stretched film containing the bacteria, and a small voltage ( $\leq 2.3$  V) was applied between the ring and two Pt wires, thus creating electrolysis. The electrolysis caused a change of the  $pH$  level in the vicinity of the electrodes, which was monitored by the addition of the indicator fluid bromothymol blue to the solution. The evolution of the  $pH$  level as a function of time is shown in Fig. 2(a), in which

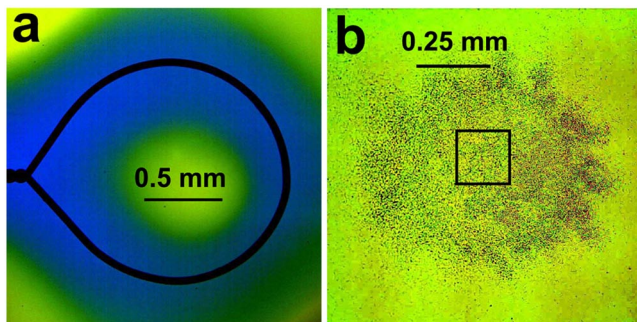


FIG. 2 (color online). (a) Image illustrating decrease of  $pH$  near the electrodes as a result of transmission of electric current. (b) Concentrated bacteria (darker part of the image). Square indicates field of view of microscope.

blue regions, corresponding to lower  $pH$  levels, expand on both sides of the ring after the application of electrical current. This expansion is due to ionic diffusion. The change of  $pH$  in turn triggers a chemotactic response in bacteria [13,14]: bacteria tend to swim away from the electrodes, towards the area of a more comfortable  $pH$  level ( $\sim 7.2$ ) in the middle of the ring [see Fig. 2(b)] and movie 1 in [15]. Quite conveniently, this technique stimulated a response only from motile bacteria; dead or otherwise nonmotile cells remain behind. With this method we are thus able to change dynamically the number density of bacteria by a factor exceeding 5. Images of the collective state were acquired from a small area  $230 \times 230 \mu\text{m}^2$  in the middle of the ring.

Selected images of bacterial patterns for different filling fractions  $\rho$  are shown in Fig. 3 (here,  $0 < \rho < 1$  is measured as a fraction of full surface coverage by bacteria). The velocity field  $\mathbf{V}$  was extracted from consecutive images by the technique of particle imaging velocimetry (PIV), the bacteria themselves serving the role of tracers (resolution about  $2 \mu\text{m}/\text{sec}$ ). Since we study rather high bacterial filling fractions of the film, traditional methods of flow visualization which utilize added passive markers are rather ineffective, as the tracers tend to adhere to the bacteria. In addition to the velocity field extracted from each image, we also measured the (reconstructed) vector field of bacterial orientations  $\boldsymbol{\tau}$ . This was done by first extracting from the images the director  $\mathbf{n}$  by finding the direction of maximal projection of an image of a bacterium

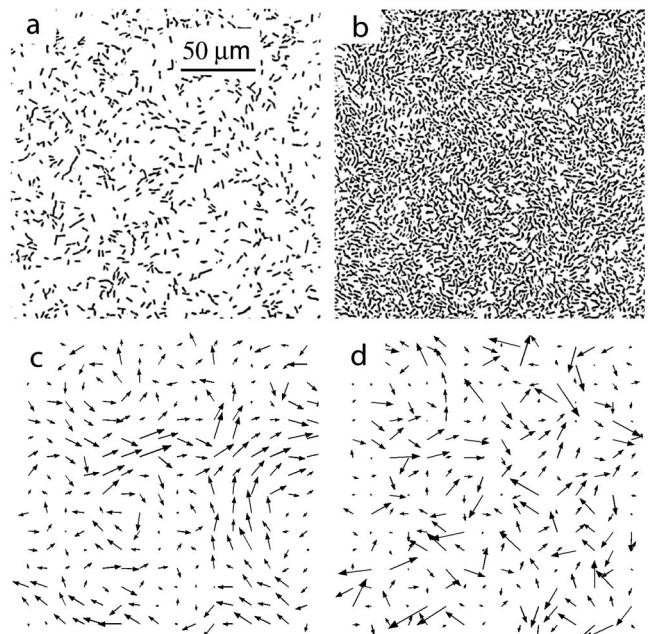


FIG. 3. Bacteria patterns for low density  $\rho = 0.14$ , no collective swimming (a); high density  $\rho = 0.47$ , well-developed chaotic large-scale flows (b). Vector fields for velocity  $\mathbf{V}$  (c) and orientation  $\boldsymbol{\tau}$  (d) for the configuration shown in image (b). See also movies 2 and 3 in [15].

on a certain direction. Then, assuming that the absolute value of the angle difference between the orientation vector  $\boldsymbol{\tau}$  and bacterial flow velocity field is smaller than  $\pi/2$ , that is,  $(\boldsymbol{\tau} \cdot \mathbf{V}) > 0$  (since bacteria swim in the direction of their orientation), one may extend the definition of the director  $\mathbf{n}$  and reconstruct uniquely the vector field  $\boldsymbol{\tau}$  [16].

In the regime of well-developed large-scale flow [Fig. 3(b)], the cross-correlation between the vector fields  $\boldsymbol{\tau}$  and  $\mathbf{V}$  over the entire span of the image yields a rather puzzling result: the correlation coefficient was smaller than 8%. However, this seeming contradiction of the fact that bacteria swim in the direction of their orientation can be resolved, for in the well-developed, chaotic flow the bacteria are advected by the fluid velocity field  $\mathbf{v}_f$  created by *all bacteria*. Since each bacterium swims in the direction of its orientation only in the *local frame* moving with fluid velocity  $\mathbf{v}_f$ , one should not expect strong global correlation between  $\mathbf{V}$  and  $\boldsymbol{\tau}$  as long as the fluid velocity field is chaotic. In contrast, there is significant correlation between the maximal values of these fields, since more oriented patches of bacteria create faster flow. In order to demonstrate this, we characterize the alignment between these two fields by the alignment coefficient  $C$ ,

$$C = \frac{\langle \cos \phi \rangle - 2/\pi}{1 - 2/\pi}, \quad (1)$$

where  $\phi$  is the angle between  $\mathbf{V}$  and  $\boldsymbol{\tau}$  (note that  $-\pi/2 < \phi < \pi/2$  due to our choice of the direction of  $\boldsymbol{\tau}$ ). If the directions between  $\mathbf{V}$ ,  $\boldsymbol{\tau}$  were random, then the value of  $\langle \cos \phi \rangle = 2/\pi$  and then  $C = 0$ , whereas perfectly aligned fields have  $C = 1$ . To amplify the contributions from large-amplitude regions of the fields  $\boldsymbol{\tau}$  and  $\mathbf{V}$  we used the following method: in the averaging procedure we exclude those points of both fields where the amplitudes were below certain variable thresholds  $V_s = k\langle |\mathbf{V}| \rangle$  or  $\tau_s = k\langle |\boldsymbol{\tau}| \rangle$ , where the parameter  $k$  measures the fraction of the mean value of each field. The alignment coefficient  $C$  vs  $k$  is shown in Fig. 4, and one sees there that the alignment indeed decreases with the density  $\rho$  due to the effect of large-scale flow discussed above. Note that bacteria at low concentration swim exactly in the direction of their orientation, and  $C \rightarrow 1$ . With the increase in  $k$ , the coefficient  $C$  indeed increases, supporting the statement that more aligned regions are also moving faster.

We performed systematic measurements of the collective flow properties over a range of bacterial number density  $\rho$  which was adjusted dynamically in the course of an experiment using the technique described above. The inset to Fig. 5 shows a typical time course of  $\rho$ . From the experimental data we extracted the typical fluid velocity  $\bar{V} = \sqrt{\langle \mathbf{V}^2 \rangle} - \langle \mathbf{V} \rangle^2$ , and the radial velocity correlation functions  $K(r)$ , defined as ( $\theta$  is a polar angle)

$$K(r) = \int d\mathbf{r}' \int_0^{2\pi} d\theta [\langle \mathbf{V}(\mathbf{r}') \cdot \mathbf{V}(\mathbf{r} + \mathbf{r}') \rangle - \langle \mathbf{V}(\mathbf{r}') \rangle^2].$$

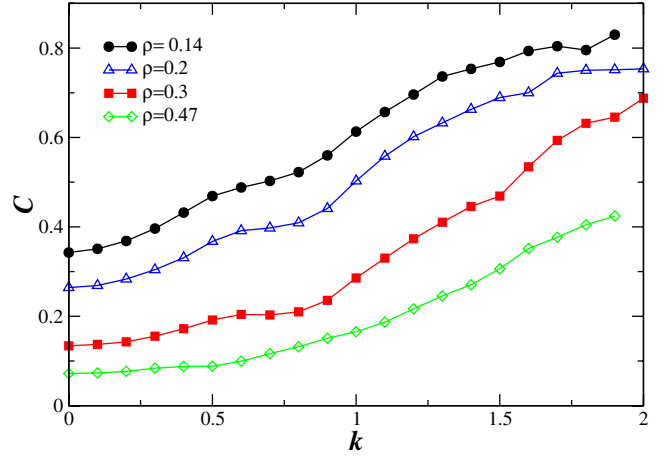


FIG. 4 (color online). Alignment coefficient  $C$  [see Eq. (1)] vs threshold  $k$  for different values of density  $\rho$ .

The correlation length was extracted from  $K(r)$  by a fit to an exponential,  $K(r) \sim \exp(-x/L) + B$ ,  $B = \text{const}$ . In most experiments the constant  $B$  was rather small, however, near the threshold the function  $K(r)$  appears to exhibit oscillations, likely due to large-scale vortex motion [17]. We also measured the orientational correlation length (not shown in Fig. 5). The results are shown in Fig. 5. While the shape of the correlation functions  $K(r)$  and the value of correlation length  $L$  are in agreement with previous measurements in Ref. [3], our results have the added benefit of not being contaminated by boundary effects and large-scale oxygen concentration gradients. Our measurements are performed in a film of constant thickness, whereas in previous works [2,3] the film thickness variations were significant.

As one sees from Fig. 5, no sharp transition occurs with increasing density; we find only a smooth (although steep)

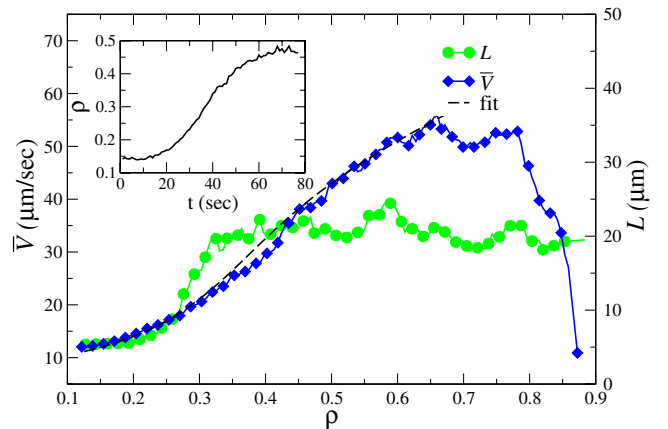


FIG. 5 (color online). Typical velocity  $\bar{V}$  (diamonds) and velocity correlation length  $L$  (circles) as the function of bacterial number density  $\rho$ . Dashed line shows fit of  $\bar{V}$  to solution to Eq. (2) with  $\rho_c \approx 0.28$ . Inset: typical dependence of density  $\rho$  vs time in the course of experiment.

increase of the velocity  $\bar{V}$  and the correlation length  $L$ . The overall changes in these quantities were about a factor of 5. For even higher density ( $\rho \rightarrow 1$ , i.e., close to 90% surface coverage) we notice complete termination of motion.

These results are distinct from predictions of the pioneering, simplified theories of collective motion in systems of self-propelled particles [6–9]. We interpret our observation as implying a smearing of a phase transition by noise which can arise from a number of sources, such as spontaneous orientation fluctuations of individual bacteria due to tumbling, small-scale hydrodynamic fluctuations due to flagellum rotation, size distribution of bacteria, etc. While we did not pinpoint the primary cause for the noise, its effect appears to be very robust and qualitatively independent on the specific nature of the fluctuations. In the accompanying theoretical paper [18] we develop a mathematical model of collective swimming. In the absence of noise the model indeed exhibits a second-order phase transition, with a divergence of the correlation length  $L$  at the critical point. However, for the strong enough noise, the transition smears, and only a smooth (although rather steep) increase of  $L$  with density  $\rho$  was observed, in qualitative agreement with these experiments. To support this observation, we compared our experimental data for  $\bar{V}$  vs  $\rho$  with those obtained from the normal form equation for a generic noisy second-order phase transition

$$\partial_t V = (\rho - \rho_{\text{cr}})V - V^3 + \zeta(t), \quad (2)$$

where  $\zeta$  is Gaussian white noise with the intensity  $D$ , and  $\rho_{\text{cr}}$  is critical density. In the absence of noise one obtains the mean-field result  $\bar{V} \sim \sqrt{\rho - \rho_{\text{cr}}}$ . With the noise one obtains a smearing of the transition point  $\rho_{\text{cr}}$ . Figure 5 shows that the fit of a solution to Eq. (2), a hypergeometric function is consistent with the experimental data (see Fig. 5).

In conclusion, we have presented experimental studies of collective bacterial swimming in thin fluid films where the dynamics are essentially two-dimensional and the concentration can be adjusted continuously. Our results provide strong evidence for the pure hydrodynamic origin of collective swimming, rather than some chemotactic mechanisms of pattern formation (chemotactic interaction, relevant for slow bacteria on a substrate, does not play any significant role in our experiment due to the very fast mixing rates in the collective flow state) [19]. For instance, the primary chemoattractant (oxygen) is expected to be highly uniform because of the thin-film geometry with air on both sides and fast stirring of fluid by the bacteria.

Swimming of bacteria in the direction of their orientation is the underlying reason for the onset of large-scale

chaotic flows. The technique utilized for the concentration and separation of bacteria by an electric field may find interesting future applications for bioanalysis and miniaturized medical diagnostic devices.

We thank Michael Graham, Frank Jülicher, Karsten Kruse, Hugues Chaté, and Eberhard Bodenschatz for useful discussions and Deborah Hanson for help. This work was supported by the DOE Grant No. DE-AC02-06CH11357 and NSF Grant No. PHY-0551742 (J. O. K. and R. E. G.).

- 
- [1] X.-L. Wu and A. Libchaber, Phys. Rev. Lett. **84**, 3017 (2000).
  - [2] N.H. Mendelson *et al.*, J. Bacteriol. **181**, 600 (1999).
  - [3] C. Dombrowski *et al.*, Phys. Rev. Lett. **93**, 098103 (2004).
  - [4] I.H. Riedel, K. Kruse, and J. Howard, Science **309**, 300 (2005).
  - [5] Ch. Becco *et al.*, Physica (Amsterdam) **A367**, 487 (2006); J. Buhl *et al.*, Science **312**, 1402 (2006).
  - [6] J. Toner and Y. Tu, Phys. Rev. Lett. **75**, 4326 (1995).
  - [7] G. Grégoire and H. Chaté, Phys. Rev. Lett. **92**, 025702 (2004).
  - [8] C. Huepe and M. Aldana, Phys. Rev. Lett. **92**, 168701 (2004).
  - [9] T. Vicsek, A. Czirók, E. Ben-Jacob, I. Cohen, and O. Shochet, Phys. Rev. Lett. **75**, 1226 (1995); A. Czirók, H.E. Stanley, and T. Vicsek, J. Phys. A **30**, 1375 (1997).
  - [10] R.A. Simha and S. Ramaswamy, Phys. Rev. Lett. **89**, 058101 (2002).
  - [11] J.O. Kessler, in *International Conference on Differential Equations*, edited by B. Fiedler, K. Gröger, and J. Sprekels (World Scientific, Singapore, 2000), Vol. 2, p. 1284.
  - [12] J.P. Hernandez-Ortiz, Ch.G. Stoltz, and M.D. Graham, Phys. Rev. Lett. **95**, 204501 (2005).
  - [13] M. Kihara and R.M. Macnab, J. Bacteriol. **145**, 1209 (1981).
  - [14] T. Minamino *et al.*, J. Bacteriol. **185**, 1190 (2003).
  - [15] See EPAPS Document No. E-PRLTAO-98-040716 for experimental movies. A direct link to this document may be found in the online article's HTML reference section. For more information on EPAPS, see <http://www.aip.org/pubservs/epaps.html>.
  - [16] In the future generation of our experiments we plan to recover the true orientation field  $\tau$  by direct identification of the flagellum position of each bacterium, and the flow velocity field, e.g., with the fluorescent microscopy.
  - [17] Typical correlation time of the collective swimming state was, as in Ref. [3], of the order of 1–2 sec.
  - [18] I.S. Aranson, A. Sokolov, J.O. Kessler, and R.E. Goldstein Phys. Rev. E **75**, 040901(R) (2007).
  - [19] F. Keller and L.A. Segel, J. Theor. Biol. **30**, 225 (1971).